THE JOURNAL OF BIOLOGICAL CHEMISTRY VOL. 282, NO. 39, pp. 28749–28758, September 28, 2007

Exocytotic Release of ATP from Cultured Astrocytes*[S]

Received for publication, January 10, 2007, and in revised form, July 11, 2007 Published, JBC Papers in Press, July 12, 2007, DOI 10.1074/jbc.M700290200

Tina Pangršič[‡§1], Maja Potokar[‡§1], Matjaž Stenovec[‡§], Marko Kreft[‡§], Elsa Fabbretti[¶], Andrea Nistri[¶], Evgeny Pryazhnikov[‖], Leonard Khiroug[‖], Rashid Giniatullin[¶], and Robert Zorec[‡§2]

From the [‡]Laboratory of Neuroendocrinology-Molecular Cell Physiology, Institute of Pathophysiology, Faculty of Medicine, University of Ljubljana, Zaloška 4, SI-1000 Ljubljana, Slovenia, the [§]Celica Biomedical Center, Proletarska cesta 4, SI-1000 Ljubljana, Slovenia, the [‖]Neuroscience Center, University of Helsinki, PO Box 56 (Viikinkaari 4), FIN-00014 Helsinki, Finland, and the [¶]Neurobiology Sector, International School for Advanced Studies (SISSA), Via Beirut 2-4, 34014 Trieste, Italy

Astrocytes appear to communicate with each other as well as with neurons via ATP. However, the mechanisms of ATP release are controversial. To explore whether stimuli that increase $[Ca^{2+}]_i$ also trigger vesicular ATP release from astrocytes, we labeled ATP-containing vesicles with the fluorescent dye quinacrine, which exhibited a significant co-localization with atrial natriuretic peptide. The confocal microscopy study revealed that quinacrine-loaded vesicles displayed mainly non-directional spontaneous mobility with relatively short track lengths and small maximal displacements, whereas 4% of vesicles exhibited directional mobility. After ionomycin stimulation only non-directional vesicle mobility could be observed, indicating that an increase in $[Ca^{2+}]_i$ attenuated vesicle mobility. Total internal reflection fluorescence (TIRF) imaging in combination with epifluorescence showed that a high percentage of fluorescently labeled vesicles underwent fusion with the plasma membrane after stimulation with glutamate or ionomycin and that this event was Ca^{2+}-dependent. This was confirmed by patch-clamp studies on HEK-293T cells transfected with $P2X_3$ receptor, used as sniffers for ATP release from astrocytes. Glutamate stimulation of astrocytes was followed by an increase in the incidence of small transient inward currents in sniffers, reminiscent of postsynaptic quantal events observed at synapses. Their incidence was highly dependent on extracellular Ca^{2+}. Collectively, these findings indicate that glutamate-stimulated ATP release from astrocytes was most likely exocytotic and that after stimulation the fraction of quinacrine-loaded vesicles, spontaneously exhibiting directional mobility, disappeared.

Many recent studies demonstrate that astrocytes play a significant modulatory role in synaptic physiology (1–4). Astrocytes respond to neurotransmitters, integrate different inputs, and signal back to neurons or forward information to neighboring or more distant astrocytes (2). In response to stimulation they release several chemical substances (5–7), termed gliotransmitters, which can interfere with the neuronal communicating pathways (8–10).

One major extracellular messenger important for coordinating the function of astrocytes, as well as for the cross-talk between them and other cell types, is ATP (11). Whereas several lines of evidence support the idea of ATP release from astrocytes (12–14), the release mechanisms are not completely understood. Some studies have described a connexin hemichannel-mediated release (12, 15, 16) in both resting and activated conditions. Other possible mechanisms, like volume-regulated anion channels (17, 18) and ATP-binding cassette transporters (multidrug resistance P-glycoprotein (19), or cystic fibrosis transmembrane conductance regulator (20) have also been reported. On the contrary, only few studies have focused on the possibility of exocytotic, vesicular ATP release mechanism operating in astrocytes (13, 14), even though it has been shown that astrocytes express the elements of the exocytotic apparatus (21–24). Furthermore, ATP has been found in secretory vesicles together with classical neurotransmitters (for instance, acetylcholine in neurons and noradrenaline in neurons and chromaffin cells (25). Therefore, it seems likely that ATP is released by the process of exocytosis from excitable cells (26, 27). In our previous studies we have described a Ca^{2+}-dependent exocytotic release mechanism of atrial natriuretic peptide (ANP)[3] and glutamate from cortical astrocytes (24, 28, 29). Before engaging in exocytosis, vesicles are transported through the cytoplasm of cells to the plasma membrane. In our recent study we have shown that transport of ANP-containing vesicles through the cytoplasm of astrocytes is supported by different types of the cytoskeleton (30).

The aim of the present study was to characterize the nature and behavior of ATP-containing vesicles in astrocytes and to further explore the properties of exocytosis as a potential mechanism of ATP release from astrocytes. To this end, we used several approaches: first, we stained ATP vesicles with quinacrine (14, 31) and examined their subcellular localization with immunocytochemistry. Second, using total internal reflection fluorescence and confocal microscopy, we analyzed vesicle mobility and their fusion with the plasma membrane after var-

* This work was supported in part by Grants Z3-7476-1683-06 of Slovenian Research Agency and P3 310, of The Ministry of Higher Education, Science and Technology of The Republic of Slovenia, BI-US/06-07-015, EC Contract DECG QLG3-CT-2001-02004, and by Center for International Mobility (CIMO), Finland, and the Academy of Finland. The work carried out at SISSA was supported by a FIRB grant (to A. N.). The costs of publication of this article were defrayed in part by the payment of page charges. This article must therefore be hereby marked "*advertisement*" in accordance with 18 U.S.C. Section 1734 solely to indicate this fact.

[S] The on-line version of this article (available at http://www.jbc.org) contains supplemental Figs. S1 and S2.

[1] These authors equally contributed to first authorship.

[2] To whom correspondence should be addressed. Tel.: 38615437020; Fax: 38615437036; E-mail: robert.zorec@mf.uni-lj.si.

[3] The abbreviations used are: ANP, atrial natriuretic peptide; EGFP, enhanced green fluorescent protein; PBS, phosphate-buffered saline; BSA, bovine serum albumin; TIRF, total internal reflection fluorescence; STIC, small transient inward currents.

ious stimulatory challenges. Third, to directly test the properties of ATP release from astrocytes, a sniffer cell approach was used. For this purpose, HEK-293T cells, co-transfected with the purinergic $P2X_3$ receptor and enhanced green fluorescent protein (EGFP), were plated onto cultured cortical astrocytes; green fluorescent HEK-293T cells were then patch-clamped to record ATP-mediated membrane currents during stimulation of neighboring astrocytes.

Our experimental evidence shows a high degree of co-localization of quinacrine-loaded vesicles and vesicles containing ANP, demonstrating a likely co-storage of ATP and ANP. We report the SNARE-dependent reduction in number of quinacrine-loaded vesicles after stimulation with ionomycin, indicating the involvement of exocytotic cargo release. The mobility of the remaining vesicles, observed in the cytoplasm, significantly decreased after stimulation of cells. Finally, in sniffer engineered HEK-293T cells plated on astrocytes we detected small transient inward currents (STICs), which likely report the quantal release of ATP from astrocytes and are reminiscent of postsynaptically detected ATP-mediated events (26). In contrast, a sustained release of ATP because of permeation of channels or transporters would result in sustained increase in inward current in HEK-293T cells, whereas transient currents similar to STICs can only be reproduced with very short (10 ms) pulses of ATP application (26). The frequency of STICs increased after astrocyte stimulation by glutamate and drastically decreased in the absence of calcium in the extracellular solution. Together, these data demonstrate that various stimuli trigger a Ca^{2+}-dependent, most likely vesicular release of ATP from astrocytes.

EXPERIMENTAL PROCEDURES

Primary Rat Cortical and Hippocampal Astrocyte Cultures—Primary cortical astrocyte cultures were prepared from the cerebral cortices of 2–3-day-old rats as described (32). Briefly, cells were grown in high glucose Dulbecco's modified Eagle's medium, containing 10% fetal bovine serum, 1 mM pyruvate, 2 mM glutamine, and 25 μg/ml penicillin/streptomycin in 5% CO_2/95% air. When cells reached confluence, they were shaken three times overnight at 200 rpm and, after each shaking, the medium was changed. The cells were then trypsinized. After reaching confluence again, they were subcultured onto 22-mm diameter poly-L-lysine-coated coverslips and used in the experiments during the following 3 days.

Hippocampi of Wistar rat embryos (E18) were removed and dissociated mechanically in a Ca^{2+}- and Mg^{2+}-free balanced salt solution (CMF-BSS) at pH 7.4, containing 137 mM NaCl, 5.36 mM KCl, 0.27 mM Na_2HPO_4, 1.1 mM KH_2PO_4, 6.1 mM glucose. After centrifugation at 1,000 rpm (200 g) for 5 min, the pellet was resuspended in culture medium (pH 7.6) containing Neurobasal medium, penicillin 100 units/ml and streptomycin 100 μg/ml. The cells were plated at a density of $1.5 \cdot 10^5$ cells/cm^2 on MatTek dishes pre-treated with poly-L-lysine. Cultures were maintained in 5% CO_2/95% air at 37 °C, allowed to grow to confluence and used at 14–21 days *in vitro*. Medium was changed every 3–4 days. Astrocytes were identified on the basis of their flat morphology and close adhesion to the substrate.

Immunocytochemistry—Prior to immunocytochemistry, cortical astrocytes were labeled with quinacrine dihydrochloride (1 μM; 15 min at room temperature). Thereafter, cells were rinsed with phosphate-buffered saline (PBS) and fixed with 2% paraformaldehyde in PBS for 15 min at room temperature. Nonspecific staining was minimized by incubating cells in blocking buffer containing 3% bovine serum albumin (BSA) and 10% goat serum in PBS at 37 °C for 1 h. The cells were stained with primary and secondary antibodies, diluted into 3% BSA in PBS and incubated at 37 °C, and then treated with Light Antifade Kit (Molecular Probes, Invitrogen). A primary antibody against ANP (1:1000; Abcam, Cambridge, UK) and a secondary antibody against rabbit IgG (Alexa Fluor 546; 1:600; Molecular Probes, Invitrogen) were used (28).

Confocal Microscopy—Images of live cortical astrocytes loaded with quinacrine dihydrochloride for detection of vesicle mobility and images of immunolabeled cells were obtained with an inverted Zeiss LSM 510 confocal microscope (Jena, Germany). After incubation in quinacrine solution as described above, cells were rinsed, supplied with extracellular solution and observed with an oil immersion objective 63 ×/NA 1.4. In the study of the mobility of cell vesicles images were recorded every 2 s. For excitation of quinacrine 488 nm line of the Ar-Ion laser was used. The fluorescence signal was band-pass filtered at 505–530 nm. For cell stimulation, 2 μM ionomycin was applied by bath superperfusion.

In immunocytochemical studies we used the 543 nm beam of the He-Ne laser to excite Alexa Fluor 546 goat anti-rabbit IgG antibody. The emission fluorescence was long-pass filtered at 560 nm. For excitation of quinacrine, the Ar-Ion laser was used, as described above.

Total Internal Reflection Fluorescence (TIRF) Microscopy—TIRF-equipped CellR (Olympus Europe, Hamburg, Germany) was used to study vesicles distribution and dynamics near the plasma membrane (33). TIRF microscopy selectively reveals membrane-proximal fluorescent molecules through use of evanescent excitation light that decays exponentially in intensity along the direction perpendicular to the glass/liquid interface to which the cells adhere (33). The exponentially decaying excitation light causes fluorescently tagged vesicles to appear progressively brighter as they move toward the interface, while the vesicles located >150–200 nm from the interface are invisible in TIRF. Conversely, the intensity of wide-field epifluorescence image of the same vesicles is insensitive to their sub-micrometer translocations in the vertical direction. The ratio between the vesicle image brightness in TIRF and its epifluorescence brightness (34) was used to estimate the percentage of vesicles docked on the plasma membrane under resting conditions. To characterize the time course of stimulus-induced docking of individual quinacrine-loaded vesicles on the basal plasma membrane, time-lapse image series were generated by taking a pair of images (TIRF and epifluorescence) every 1–5 s. Vesicle docking was detected as an increase in its TIRF fluorescence with epifluorescence unchanged. Fusion of a vesicle and release of its content into extracellular space was detected as a signal loss both in TIRF and epifluorescence.

Vesicle Tracking and Co-localization Analysis—Vesicle mobility was analyzed with ParticleTR software (Celica,

Ljubljana, Slovenia) as previously described (35). We calculated the following parameters of vesicle mobility: current time (time from the beginning of single vesicle tracking), step length (displacement of a vesicle in each time interval), track length (the total length of the analyzed vesicle pathway), maximal displacement (a measure of the net translocation of a vesicle) and the directionality index (maximal displacement/total track length) of vesicles as described previously (35, 36). The analysis of vesicle mobility was performed for epochs of 30 s.

The analysis of the co-localization degree between fluorescent pixels labeling different vesicles was performed with ColoC software (Celica, Ljubljana, Slovenia). Briefly, the software counts the number of green, red and co-localized pixels in each image. The degree of co-localization used in the analysis was expressed as the degree (%) of co-localized pixels in the cell in comparison to all green pixels in the cell, which are labeling ATP-containing vesicles. Overlaid green and red signals, indicating the co-localization between the ATP and peptide hormones, were observed as a yellow color in the images.

Co-cultures of Astrocytes and Transfected HEK-293T Cells—Primary astrocyte cultures were prepared as mentioned above. Astrocytes were plated on poly-L-lysine-coated coverslips on the day of HEK-293T cell transfection.

HEK-293T cells, obtained from the SISSA cell bank, were maintained in culture using the medium for astrocytes. Co-transfection of HEK-293T cells with plasmids encoding for mutated rat $P2X_3$ receptor (provided by SISSA) and for GFP (EGFP-N1, Clontech, Takara Bio Europe, Saint-Germain-en-Laye, France) was performed using the calcium phosphate transfection method (37). For these experiments, we used the $rP2X_3$ receptor mutated at D266A to exploit the fact that, because this mutant shows very reduced desensitization (37), it greatly improves the detection of ATP-evoked current responses. HEK-293T cells were trypsinized 24 h after transfection and replated on top of astrocytes attached to coverslips. Apyrase (1 unit/ml) was added to coverslips to prevent excessive stimulation of transfected HEK-293T cells by ambient ATP. Co-cultures were used within the next 2 days after $P2X_3$-expressing HEK-293T cell plating.

The successfulness of co-transfection of $P2X_3$ and EGFP was tested by immunofluorescence experiments. Paraformaldehyde-fixed co-trasfected HEK-293T cells were processed with anti-$P2X_3$ receptor antibody (dilution 1:200, Alomone, Jerusalem, Israel) and an AlexaFluor 594-conjugated anti-rabbit secondary antibody (dilution 1:500, Molecular Probes, Invitrogen). In addition, cell nuclei were stained with DAPI. If not otherwise mentioned, all chemicals were obtained from Sigma.

Electrophysiological Recordings and Analysis—Coverslips with co-cultures of astrocytes and HEK-293T cells were bathed in extracellular medium containing (in mM): NaCl 152, KCl 5, $MgCl_2$ 1, $CaCl_2$ 2, Na HEPES 10, D-glucose 10, pH adjusted to 7.4 with NaOH. Patch-clamp pipettes had a resistance of 2–5 MΩ and were filled with (in mM): CsCl 130, $MgCl_2$ 1, HEPES 20, Na_2ATP 3, pH adjusted to 7.2 with CsOH. All recordings were made at room temperature.

Whole cell patch-clamp recordings were performed with SWAM IIB (Celica, Ljubljana, Slovenia). Green fluorescent $P2X_3$-expressing HEK-293T cells lying on top of or beside astrocytes were voltage clamped at −60 mV. Whole cell currents were acquired at 10 kHz, filtered at 1 kHz, and digitized by WinWCP software (Strathclyde University, Glasgow, UK). Off-line data analysis was performed using software subroutines written in MATLAB (MathWorks Inc.) with additional digital filtering as required. Slow drifts/fluctuations in the signal were digitally subtracted. We measured peak amplitude, rise time (20–80% of the peak amplitude) and half-decay time (to 50% of the peak amplitude) of transient current events and their apparent inter-event interval. To stimulate ATP release from astrocytes 100–300 μM glutamate was added to the extracellular solution.

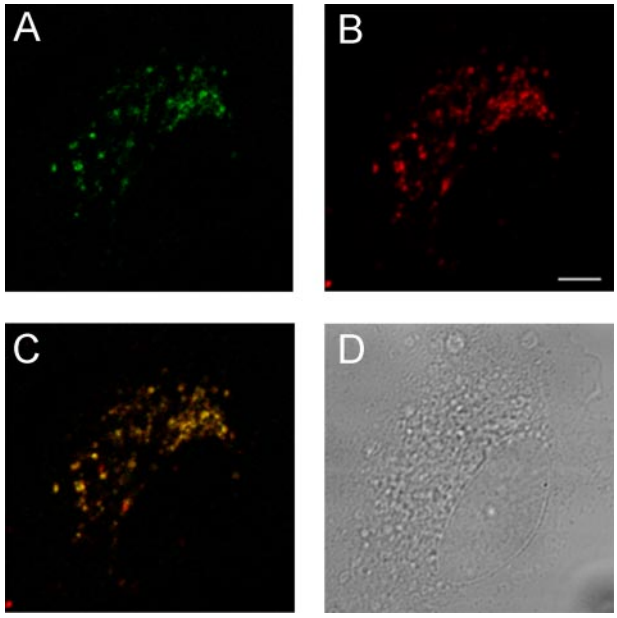

FIGURE 1. **ATP is co-stored in peptidergic vesicles of astrocytes.** Rat astrocytes were labeled with quinacrine dihydrochloride (1 μM, 15 min, room temperature) and immunolabeled with antibodies against atrial natriuretic peptide (anti-ANP, 1: 1000). Fluorescently labeled vesicles containing ATP (quinacrine dihydrochloride labeling, *green*) (*A*) and fluorescently immunolabeled vesicles containing ANP (*red*) in the same astrocyte (*B*). *C*, merged image shows a high degree of co-localization between both fluorescence signals, seen as *yellow*. The degree of fluorescence co-localization in this cell is 42%. *D*, differential interference contrast image of the same cell. *Bar*, 5 μm.

All data are given as mean ± S.E.; *n* denotes the number of individual cells assessed in patch-clamp studies or the number of events detected. Statistical differences were determined by two-tailed unpaired Student's *t* test and considered significant at $p < 0.05$.

RESULTS

Quinacrine Loading into ATP Vesicles in Astrocytes—To visualize ATP-containing vesicles in astrocytes we incubated cultures in 1 μM quinacrine dihydrochloride (14, 31). Fig. 1, displaying one section of a rat astrocyte, shows the presence of large numbers of ATP vesicles (~80 vesicles/cell), which are randomly distributed over the cell profile. To identify the nature of ATP-containing vesicles, treated cells were immunolabeled with antibodies against ANP (Fig. 1). The double staining revealed a high degree of co-localization between two dyes (*green* for quinacrine, see Fig. 1*A*, and *red* for anti-ANP, see Fig. 1*B*), observed as yellow fluorescence (Fig. 1*C*). The average

degree of quinacrine and ANP co-localization between containing vesicles, expressed as the ratio between all co-localized pixels and all green pixels in the cell, was 39.48 ± 6.59% ($n = 12$; n represents the number of analyzed cells). These results show that ATP was substantially co-stored in peptidergic vesicles with ANP in astrocytes.

The Mobility of Quinacrine-loaded Vesicles Decreased after Stimulation—The total number of tracked quinacrine-stained vesicles was 817 in non-stimulated cells ($n = 10$), while in ionomycin-stimulated (2 μM, 1 min) cells ($n = 6$) only 109 vesicles could be tracked after bath application of the Ca^{2+} ionophore. When ionomycin was omitted from the bath, the total image fluorescence (supplemental Fig. S1*A*, *filled bars*) and the number of quinacrine-stained vesicles per cell did not change significantly over time (supplemental Fig. S1*B*, *filled bars*). On the contrary, when cells were stimulated by 2 μM ionomycin, the total image fluorescence decreased from 100% to 93.8 ± 2.3% (mean ± S.E., $n = 6$) within 1 min (supplemental Fig. S1, *open bars*) and the number of quinacrine-stained vesicles decreased from 110 ± 13 to 93 ± 10 vesicles per cell (from 100% to 84.6 ± 3.0%) ($p < 0.05$, paired Student's t test). Following 2 min of incubation in the presence of ionomycin, the total image fluorescence decreased to 87.4 ± 3.7% and the number of quinacrine-stained vesicles decreased to 84 ± 10 vesicles per cell (the relative number of vesicles was reduced to 76.6 ± 5.2%), (supplemental Fig. S1, *open bars*), which is consistent with the Ca^{2+}-dependent, exocytotic fluorescent cargo release from quinacrine-stained vesicles in stimulated astrocytes. To further test that these results reflect exocytotic cargo release from quinacrine-stained vesicles as considered previously (10, 14), astrocytes were transfected with a construct to express the dominant-negative SNARE domain peptide, which blocks the formation of the SNARE complex (24). Transfected cells displaying cytosolic EGFP fluorescence were stained with quinacrine and stimulated by 2 μM ionomycin to trigger Ca^{2+}-dependent exocytosis. In transfected cells, the number of quinacrine-stained vesicles per cell was not reduced significantly ($p > 0.05$, paired Student's t test) following ionomycin stimulation (supplemental Fig. S1*B*, *gray bars*) clearly indicating that the decrease in quinacrine-stained vesicles is a SNARE-dependent process.

To estimate the mobility these vesicles were tracked for 30 s in resting conditions and from 30 to 60 s after the addition of 2 μM ionomycin. Vesicles in resting conditions predominantly displayed non-directional mobility as only a few vesicles had almost rectilinear directional mobility (Fig. 2*A*). Directional and non-directional mobility was determined as described (35).

Ionomycin application greatly affected both types of vesicle mobility. In non-stimulated cells, the maximal displacement of directional vesicles (n_d) was 2.49 ± 0.38 μm ($n_d = 35$) and the track length was 3.46 ± 0.37 μm. Following ionomycin application, none of tracked vesicles displayed directional mobility within 30–60 s after stimulation (note the absence of rectilinear tracks in Fig. 2*B*). However, ionomycin also significantly affected the mobility of non-directional vesicles. The maximal displacement of non-directional vesicles was significantly reduced from 0.37 ± 0.01 μm ($n_n = 782$); (n represents the number of vesicles) in non-stimulated cells to 0.30 ± 0.01 μm in

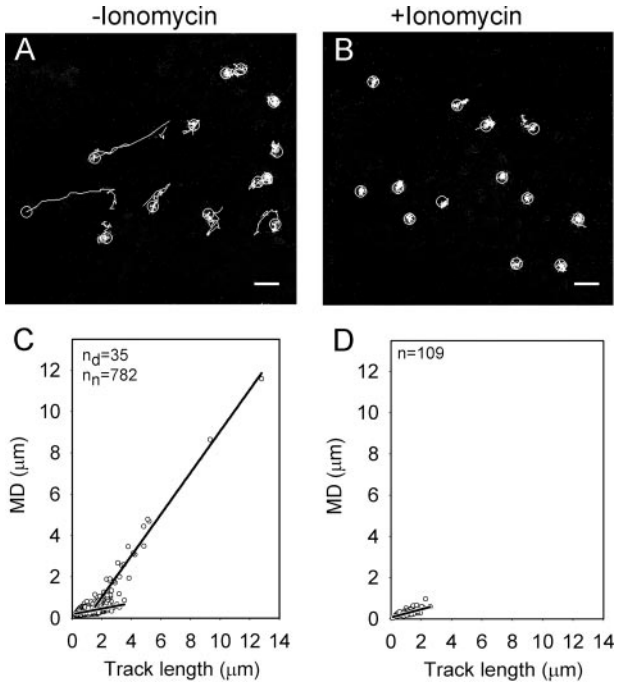

FIGURE 2. **Ionomycin reduces the mobility of ATP-containing vesicles.** *A* and *B*, circles denote starting points of vesicles, the mobility of which was analyzed for 30 s. *Bars*, 2.5 μm. In non-stimulated cells (*A*), a few vesicles display directional mobility (tracks appear almost rectilinear), whereas in ionomycin-stimulated cells (*B*) all vesicles display non-directional mobility only (absence of rectilinear tracks). *C* and *D*, relation between maximal displacement (*MD*) and length of vesicle tracks (*Track length*) in non-stimulated cells (*C*) and in ionomycin-stimulated cells (*D*). A linear function was fitted to the data in the form: [$MD = MD_0 + a \times$ (Track length)]. The slopes (*a*) of the lines fitted were 1.00 ± 0.03 for directional vesicles in non-stimulated cells (*C*), significantly different from the lines of non-directional vesicles in non-stimulated cells (0.13 ± 0.01; *C*) and 0.20 ± 0.02 for vesicles in stimulated cells (*D*). (n = number of vesicles, n_d = number of directional vesicles, n_n = number of non-directional vesicles).

ionomycin-stimulated cells, ($n = 109$; $p < 0.001$). Similarly, the mean vesicle track length was significantly shorter in stimulated (1.14 ± 0.04 μm; $n = 109$) than in non-stimulated cells (1.30 ± 0.02 μm; $p < 0.001$). Directionality index (see "Experimental Procedures") decreased from 0.66 ± 0.03 (n_d) and 0.34 ± 0.001 (n_n) to 0.28 ± 0.001 in stimulated cells. Following the elevation of free cytosolic $[Ca^{2+}]$ by ionomycin, vesicles are likely kept within specific cell domains for a prolonged period of time.

Maximal displacement was then plotted against track length and a linear function was fitted to the data using the equation with the form: [$f = y0 + a \times x$] (Fig. 2, *C* and *D*, representing the data for non-stimulated and stimulated cells, respectively). The slope of the regression line of directional vesicles (1.00 ± 0.03) is significantly ($p < 0.0001$) different from the slopes of the regression line of non-directional vesicles in non-stimulated (0.13 ± 0.01) and of vesicles in stimulated cells (0.20 ± 0.02).

Collectively, confocal microscopy of ionomycin-stimulated cells revealed that quinacrine-loaded vesicles in stimulated astrocytes displayed only non-directional mobility (Fig. 2). This was further indicated by the ionomycin-induced decrease in the maximal displacement and total track length of vesicles.

Time Course of Docking and Fusion of ATP-containing Vesicles—To visualize and quantify the time course of vesicle docking to and fusion with the plasma membrane, we applied

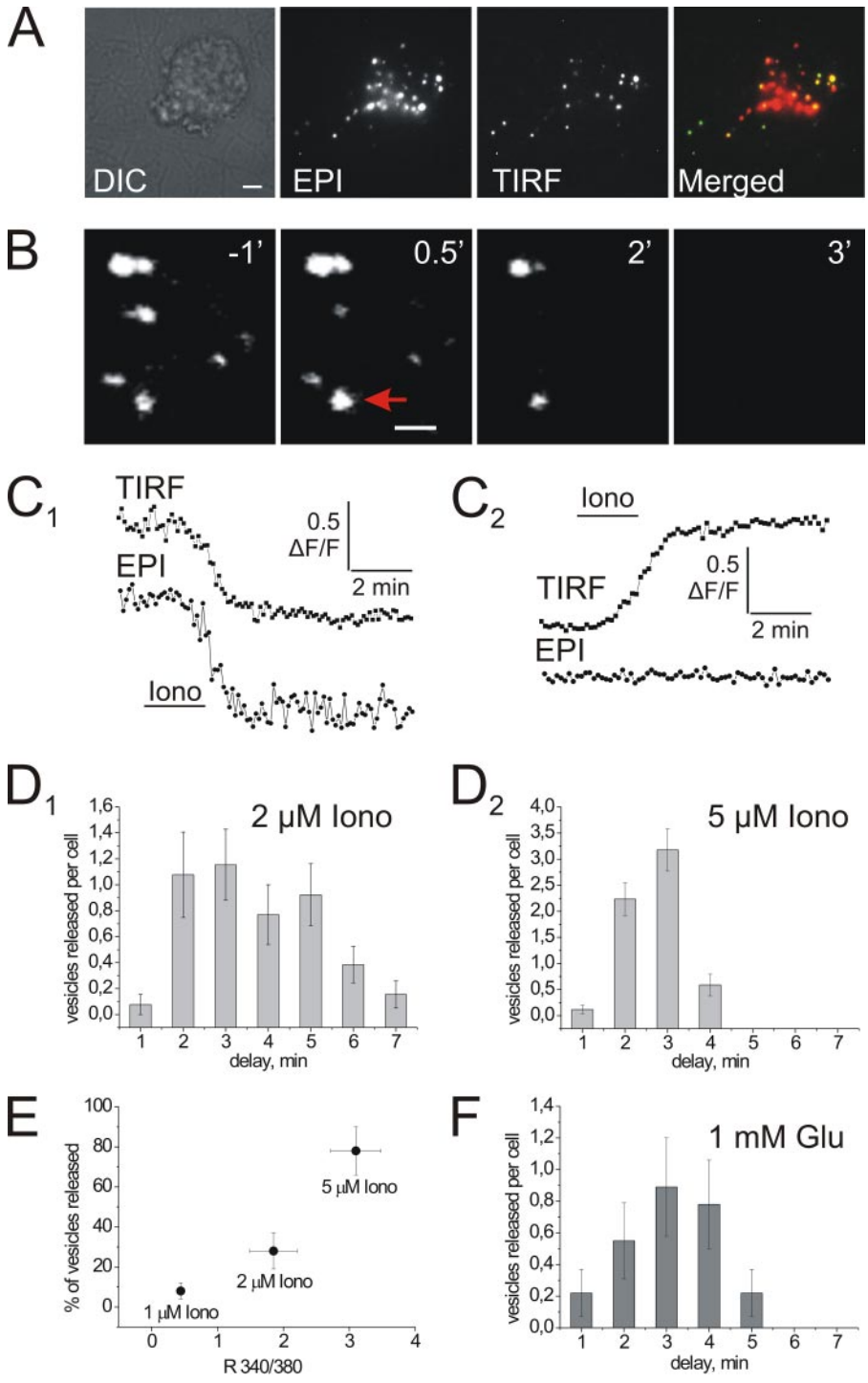

FIGURE 3. **Vesicular release of ATP studied with TIRF microscopy.** *A*, quinacrine-loaded cultured astrocytes in differential interference contrast (*DIC*), epifluorescence (*EPI*), TIRF and merged TIRF and epifluorescence (*green* and *red*, respectively) modes. Some vesicles are seen only in epifluorescence, indicating that they are not docked on the basal plasma membrane. *Bar*, 1 μm. *B*, in response to 2 μM ionomycin (applied for 2 min at time 0), most vesicles showed a decrease in their TIRF intensity as they were released, while some vesicles (such as the one indicated by the *red arrow*) showed an increase in TIRF as they docked at the plasma membrane prior to their release. *Bar*, 1 μm. *C*, examples of two types of vesicle behavior in response to ionomycin stimulation as detected with TIRF (*upper*) and Epi (*lower*) intensity time courses: *C1*, a vesicle undergoing exocytosis as evidenced by simultaneous loss of TIRF and epifluorescence signals; *C2*, a vesicle approaching the basal plasma membrane (docking) without subsequent release, as no change in epifluorescence was observed. *D*, histogram showing distribution of the delay between stimulus onset and vesicle release in response to 2 μM ionomycin (*D1*; $n = 13$) or 5 μM ionomycin (*D2*; $n = 17$). *Error bars* indicate S.E. *E*, calcium-dependent exocytosis of the ATP-containing vesicles induced by ionomycin (1, 2 or 5 μM). *Error bars* represent S.E. for $[Ca^{2+}]_i$ (*horizontal bars*) and vesicle fraction (*vertical bars*). *F*, histogram showing distribution of the delay between stimulus onset and vesicle release in response to stimulation with 1 mM glutamate. *Error bars* indicate S.E.

TIRF microscopy to quinacrine-loaded cultured hippocampal astrocytes. In resting conditions, 75 ± 5% of vesicles were detectable both in TIRF and epifluorescence mode, while the remaining 25% were only visible in epifluorescence (Fig. 3*A*). This indicates that about three quarters of ATP-containing vesicles were located in the close vicinity (within ~100–150 nm) of the plasma membrane, and perhaps formed a large pool of readily releasable docked vesicles. When ionomycin was added to the perfusion solution (2 μM for 2 min, $n = 13$ cells), 28 ± 9% of the vesicles visible in TIRF showed a loss of fluorescence in both TIRF and epifluorescence modes, which indicated the release of the vesicle and diffusion of its content (quinacrine and, presumably, ATP bound to quinacrine) into the extracellular space (38). Fig. 3*B* provides examples of individual vesicle behavior in response to stimulation with 2 μM ionomycin. The vast majority (95%) of the released vesicles displayed a simultaneous decrease in both TIRF and epifluorescence signal after a delay of up to several minutes (Fig. 3*C1*). For a small fraction of released vesicles (4%), treatment with ionomycin first caused an increase in their TIRF signal followed by decrease and eventual disappearance, indicating vesicle docking prior to exocytosis. An example of such vesicle behavior is shown in Fig. 3*B*, and the vesicle with increased fluorescence is indicated by the *arrow*. Interestingly, a very small fraction (~1%) of the vesicles visible in TIRF mode in response to ionomycin application underwent a steady increase in the TIRF signal (Fig. 3*C1*) which was not followed by fluorescence loss during the observation time. This finding indicates that a rise in $[Ca^{2+}]_i$ might trigger vesicle docking without subsequent exocytosis, at least for the duration of our recordings (15–20 min). In 13 cells tested, the delay between ionomycin-induced $[Ca^{2+}]_i$ rise (which developed in ~20 s as monitored using Fura-2 imaging; data not

shown) and release of ATP-containing vesicles was highly variable ranging from 2 to 7 min (Fig. 3*D1*). Application of a higher dose (5 μM; $n = 17$ cells) of ionomycin induced a larger $[Ca^{2+}]_i$ rise and a more pronounced (Fig. 3*E*) and coordinated release of quinacrine-loaded vesicles within the first 2–3 min upon stimulation (Fig. 3*D2*).

To test whether the same pattern of ATP release could be produced by endogenous substances, we stimulated astrocytes with glutamate, one of the main gliotransmitters (2). Glutamate-stimulated ATP release from astrocytes and the time course of the underlying vesicle fusion to plasma membrane are shown in Fig 3*F*. Bath application of glutamate (100–1000 μM for 1 min) readily induced a reversible $[Ca^{2+}]_i$ rise (data not shown) and release of ATP-containing vesicles within 5 min upon stimulation (Fig. 3*F*). Overall, 10 ± 4% of the vesicles visible in TIRF were released in response to glutamate stimulation ($n = 10$ cells). Thus, glutamate stimulation appeared to be less efficient than ionomycin to trigger ATP release (Fig. 3*E*). A small fraction of the released vesicles (4.7%) underwent docking prior to release. Preincubation with 50 μM BAPTA AM completely blocked glutamate-induced release of ATP-containing vesicles in 3 out of 3 experiments (data not shown), indicating that release was Ca^{2+}-dependent (see below).

Taken together, the TIRF imaging experiments have revealed that: 1) the majority of ATP-containing vesicles were docked on plasma membrane in resting cultured astrocytes, and 2) stimulus-induced $[Ca^{2+}]_i$ rise triggered fusion of these vesicles to the plasma membrane within 3–5 min suggesting a relatively slow release mechanism when compared with neurons (29, 39, 40).

Detection of Quantal ATP Release by Sniffer HEK-293T Cells—To detect the release of ATP from cortical astrocytes, HEK-293T cells expressing the mutated (D266A) $P2X_3$ receptor (37) were used as ATP "sniffer" cells. $P2X_3$ receptor is not natively expressed in HEK-293T cells (41). The single-point mutation of $P2X_3$ within the subunit ectodomain preserves high affinity agonist binding together with less desensitization (37). Because wild-type receptors rapidly desensitize, this mutation is, considerably advantageous for ATP sniffing. To facilitate identification of potential sniffers, HEK-293T cells were co-transfected with EGFP. Immunofluorescence experiments using antibody against the $P2X_3$ receptor were performed to verify that both constructs were properly co-expressed in the same cell. As shown on Fig. 4, *A–C* in the great majority of cases (>80%) green cytoplasmic fluorescence of EGFP and red plasmalemmal anti-$P2X_3$ receptor fluorescence coincided within the same cell. Thus, successfully transfected HEK-293T cells expressing $P2X_3$ receptors could be readily identified in culture as green fluorescent cells.

Next, $P2X_3$-EGFP transfected HEK-293T cells were plated onto cortical astrocytes. Green fluorescent HEK-293T cells, which were lying on top of or in close proximity of astrocyte(s) were used as ATP sniffer cells. An example of such cell arrangement is shown in Fig. 4*D*. ATP sniffer cells were patch-clamped in whole cell configuration. In resting conditions, 8 of 10 sniffer cells displayed spontaneous STICs (Fig. 5*A*), probably indicating the spontaneous ATP release from astrocytes because such current changes were not detected in transfected HEK-293T cells cultured without astrocytes. The mean amplitude of

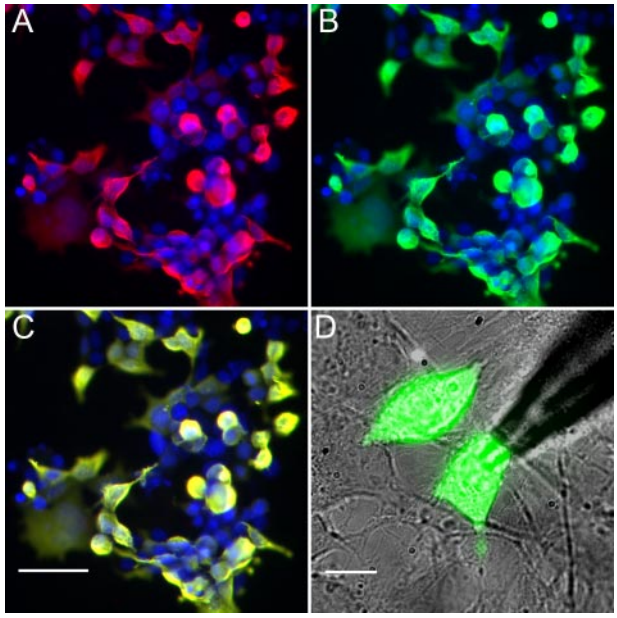

FIGURE 4. **Co-expression of transfected EGFP (*green*) and $P2X_3$ receptors (*red*) in HEK-293T cells and coculture of astrocytes and transfected HEK-293T cells.** *A–C*, HEK-293T cells, co-transfected with EGFP and $P2X_3$ receptor and processed by anti-$P2X_3$ receptor antibody. Fluorescent image of anti-$P2X_3$ receptor antibody-secondary antibody complex (*red*, *A*), expressed EGFP (*green*, *B*), and merged image (*C*), showing an overlap of green and red fluorescence signal. Cell nuclei were stained by DAPI (*blue*, *A–C*). *Bar*, 50 μm. *D*, fluorescent and transmission image of green fluorescent $P2X_3$-expressing HEK-293T cell lying on top of an astrocyte monolayer. Note the patch pipette in the *upper right corner*. *Bar*, 10 μm.

STICs in resting conditions was 6.62 ± 0.71 pA, with a rise time (20–80%) of 0.18 ± 0.03 s and half-decay of 2.25 ± 0.22 s ($n = 8$ cells).

In keeping with TIRF microscopy data, in sniffer experiments ATP release from astrocytes was also elicited by the gliotransmitter glutamate. When HEK-293T cells were plated alone, glutamate (100 or 300 μM) failed to evoke any STICs (data not shown). In contrast, in co-cultures with astrocytes, the incidence of STICs increased after application of glutamate in all experiments (Fig. 5*A*), indicating that the release of ATP from astrocytes was involved. We analyzed the responses of 10 sniffer HEK-293T cells that displayed STICs after the application of glutamate. While the amplitude, rise time and half-decay of STICs did not change significantly, the analysis of temporal distribution of STICs revealed a significant decrease in average inter-event interval in stimulated conditions (Fig. 5*B*, *asterisk*, $p < 0.05$). The amplitude and half-decay of STICs were independent as shown by the lack of correlation between these two parameters (Fig. 5*C*; linear regression, $r = 0.41$ and 0.38 (before and after stimulation, respectively), $p > 0.05$). We have additionally tested the origin of STICs by applying A-317491, a highly selective $P2X_3$ receptor antagonist (10 μM, Sigma, Milan; 42, 43), to the bathing medium. Whereas STICs were observed before and after adding glutamate to control bathing medium (supplemental Fig. S2), application of A-317491 almost completely abolished their occurrence. In 749 s following the addition of the antagonist, we found only 3 STICs even if additional glutamate was present in the bath medium (supplemental Fig. S2; *white asterisk* in the bar marks the

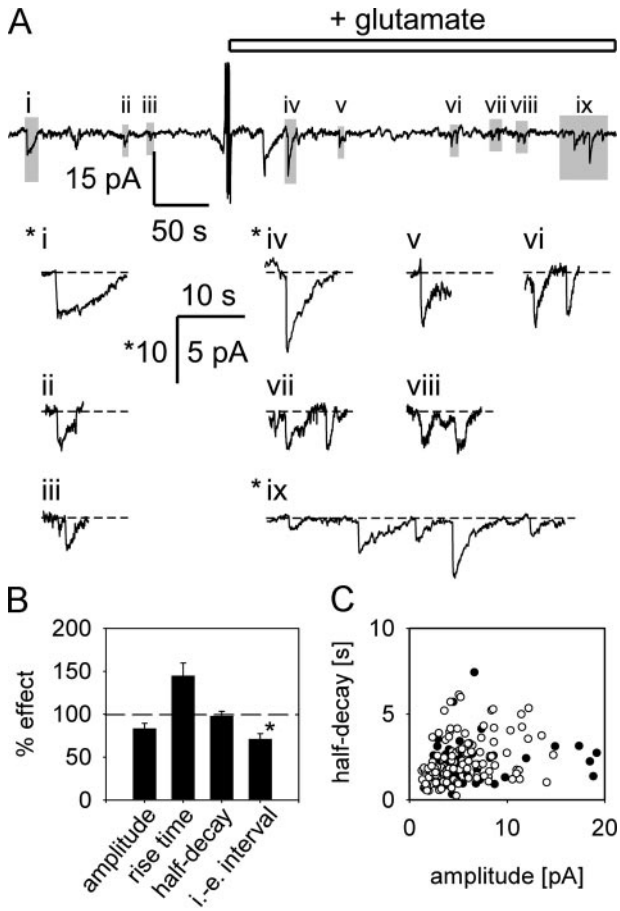

FIGURE 5. **Detection of small transient inward currents (STICs) in HEK-293T cells cultured on astrocytes.** *A*, membrane current recorded from voltage-clamped HEK-293T cell (co-expressing EGFP and $P2X_3$) lying on an astrocyte. STICs are observed before and after the addition of glutamate (300 μM; *bar*) to the bathing medium. *Below*, regions with the observed STICs (*gray rectangles*) are shown on an expanded current scale (i-ix). In resting conditions 3 STICs (i-iii) appear and, after addition of glutamate, 13 STICs of variable amplitudes (in regions iv-ix) are detected. Note the difference in current scale for inset i, iv, and ix (10 pA, *asterisks*) as compared with 5 pA for insets ii, iii, and v-viii. *B* and *C*, properties of STICs. *B*, while the addition of glutamate evoked no significant change in the peak amplitude, rise time, or half-decay of STICs, a significant decrease in the mean inter-event interval of STICs was detected. The values are normalized to the mean parameter values of events detected in resting conditions. The normalized peak amplitude, rise time, half-decay, and inter-event interval after application of glutamate are 83.41 ± 6.00, 144.91 ± 14.81, 97.83 ± 5.43, and 71.13 ± 6.35%, respectively (*, $p < 0.05$, *t* test). *Error bars* indicate mean ± S.E. *C*, plot of half-decay *versus* peak amplitude of STICs reveals the lack of correlation between the two parameters (before stimulation (*white circles*): $r = 0.41$, $n = 56$; after stimulation (*black circles*): $r = 0.38$, $n = 145$). *n* denotes the number of STICs, detected in all experiments.

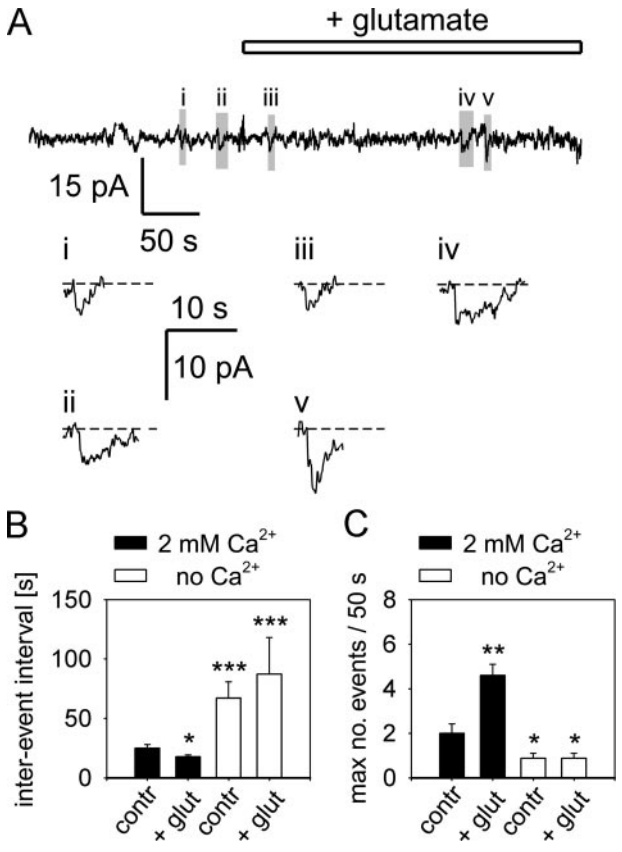

FIGURE 6. **STICs occur in a Ca^{2+}-dependent manner.** *A*, membrane current recorded from voltage-clamped HEK-293T cell (co-expressing EGFP and $P2X_3$) lying on astrocytes. Cells are bathed in Ca^{2+}-free extracellular solution containing 5 mM EGTA. Only very few STICs are observed before and after the addition of glutamate (300 μM; *bar*) to the bathing medium in Ca^{2+}-free conditions. *Below*, regions with the observed STICs (*gray rectangles*) are shown on an expanded current and time scale (i-v). In resting conditions 2 STICs (i-ii) are detected and, after addition of glutamate, 3 (iii-v). *B* and *C*, in Ca^{2+}-free extracellular solution only very few STICs are detected in resting (contr) as well as in glutamate-stimulated (+*glut*) conditions. *B*, histogram shows the mean inter-event interval in standard extracellular solution (containing 2 mM Ca^{2+}, *black bars*): 24.87 ± 3.17 s ($n = 48$) before, 17.69 ± 1.58 s ($n = 135$) after addition of glutamate; and in Ca^{2+}-free solution (*white bars*): 67.07 ± 13.82 s ($n = 8$) before, 87.21 ± 30.84 s ($n = 8$) after addition of glutamate. *n* denotes the number of inter-event intervals in all experiments detected. *C*, histogram of the maximal number of events detected in the 50-s time frame in standard extracellular solution (*black bars*): 2.00 ± 0.42 ($n = 10$) before, 4.60 ± 0.50 ($n = 10$) after addition of glutamate; and in Ca^{2+}-free solution (*white bars*): 0.88 ± 0.23 ($n = 8$) before, 0.88 ± 0.23 ($n = 8$) after addition of glutamate. *n* denotes the number of experiments. *Asterisks* denote a statistically significant difference between the controls in standard solution and the other experiments (*, $p < 0.05$; **, $p < 0.001$; ***, $p < 0.0001$).

time of second glutamate application). In a batch of 6 cells, no STICs were detected either prior to or after adding glutamate to the medium containing A-317491. The characteristics of the responses recorded in our experiments on sniffer cells are consistent with the view that they express quantal release of ATP from astrocytes (26).

The Release of ATP from Cortical Astrocytes Was Ca^{2+}-dependent—To provide further insight into the mechanism of ATP release from astrocytes, the dependence on extracellular Ca^{2+} was tested using sniffer cells. To explore the Ca^{2+} dependence of STICs, we first bathed the cells in Ca^{2+}-free extracellular solution containing 5 mM EGTA. In Ca^{2+}-free solution much fewer STICs were detected in resting conditions (Fig. 6*A*), suggesting that the spontaneous release of ATP from astrocytes was, at least in part, triggered by influx of extracellular Ca^{2+}. In two out of 8 $P2X_3$-expressing HEK-293T cells, no STICs were observed before adding glutamate. Furthermore, in all cells tested in Ca^{2+}-free medium, the application of 300 μM glutamate did not affect the incidence of STICs (Fig. 6*A*), clearly indicating their dependence on extracellular Ca^{2+}. The analysis of the inter-event interval measured in 6 sniffer cells in resting conditions and in 5 cells after application of glutamate shows a significant increase in the inter-event interval in resting as well as in stimulated Ca^{2+}-free conditions (67.1 ± 13.8 s, $n =$ 8 inter-event intervals from 6 cells, and 87.2 ± 30.8 s, $n = 8$

inter-event intervals from 5 cells, respectively; Fig. 6*B*) as compared with the inter-event interval measured in resting conditions in standard extracellular solution (24.87 ± 3.17, $n = 48$ inter-event intervals from 8 cells; $p < 0.0001$; Fig. 6*B*). Because the inter-event interval could not be measured in all cells (some displayed only one if any STIC in the recorded time), we performed additional analysis by counting the number of events detected in a shifting 50 s time frame. The maximal number of events detected in any of the time frames is shown in the histogram of Fig. 6*C*. In standard extracellular solution the maximal number of events in a 50 s epoch increased from 2.00 ± 0.42 ($n = 10$) in resting conditions to 4.60 ± 0.50 ($n = 10$, where n denotes the number of experiments; $p < 0.001$) after addition of glutamate. In contrast, the maximal number of events in Ca^{2+}-free solution was statistically lower both before (0.88 ± 0.23, $n = 8$) and after the application of glutamate (0.88 ± 0.23, $n = 8$, where n denotes the number of experiments) as compared with the maximal number of events detected in resting conditions in standard extracellular solution ($p < 0.05$; Fig. 6*C*).

The shape of glutamate-induced STICs very much resembled the events detected by Fabbro *et al.* (26) although with somehow slower kinetics (longer rise and decay time) which presumably indicated lower affinity of $P2X_2$ *versus* $P2X_3$ receptors (44) and the larger impact of diffusion processes on the amplitude and time shaping of the currently observed STICs.

DISCUSSION

In the current study we aimed at exploring the nature of stimulated ATP release from astrocytes together with any potential change in the mobility of astrocytic vesicles.

It has been suggested that ATP in astrocytes may be co-stored within vesicles with glutamate (2) or peptides (31). By exploiting the fact that quinacrine binds ATP in peptidergic vesicles, we show that in ~40% of vesicles ATP was stored in secretory vesicles together with peptides such as ANP. Next, the mobility of quinacrine-loaded vesicles was examined by using confocal microscopy, enabling us to study the mobility of all vesicles in the cytoplasm, including those not detected by TIRF. In our previous study we have shown that ANP-containing vesicles in cortical astrocytes display two types of mobility (35), whereby 35% of vesicles exhibited directional mobility. Interestingly, the quinacrine-loaded vesicles of the present study predominantly showed non-directional mobility with <1 μm maximal displacement. Only ~4% of vesicles in non-stimulated cells displayed directional mobility. Whether vesicle mobility is observed as directional or non-directional likely depends on their pattern of attachment to the cytoskeleton (35, 45, 46).

Like in our previous study (35), we observed no difference in the apparent shape or size of vesicles in both groups. The mechanism of spontaneous mobility of quinacrine-loaded vesicles is not known. Because most of them were non-directional, we propose that their mobility mainly involved free diffusion (30, 35). Stimulation with ionomycin significantly reduced maximal displacement and total track length of all vesicles. Further, the average directionality index (ratio between maximal displacement and the total track length) decreased. This finding is interesting because some previous studies showed no effect of increased $[Ca^{2+}]_i$ on vesicle mobility (secretory granules in PC12 cells (47), peptidergic vesicles containing ANP.Emd, atrial natriuretic peptide, tagged with green fluorescent protein (48) in cortical astrocytes (30)). In contrast, a study on insect neuromuscular junction also reports the sensitivity of vesicular mobility to activity-induced Ca^{2+} influx (49). However, ANP-containing vesicles in that study were immobile before stimulation and exhibited unidirectional movement only after stimulation (49). Arrested trafficking of peptidergic vesicles may impact cargo delivery throughout the cell cytoplasm and to the plasma membrane, which may potentially impair long-term secretory activity. However, if vesicles are at the fusion site (most vesicles were, indeed, visible with TIRF microscopy in our experiments, Fig. 3), the arrested mobility may increase the probability of observing an open fusion pore, perhaps resulting in an increased open fusion-pore dwell-time. The overall decrease in the total image fluorescence and in the number of quinacrine-stained vesicles after ionomycin-treatment in this study suggests that a significant number of fluorescent vesicles underwent exocytosis.

The latter observation was further confirmed by TIRF studies, which showed a decrease in fluorescence of quinacrine-loaded vesicles upon stimulation with either ionomycin or the gliotransmitter glutamate. The majority of observed vesicles appeared to be docked at the plasma membrane in resting conditions because (*a*) most of them were visible in TIRF prior to stimulation and (*b*) both epifluorescence and TIRF signal decreased after stimulation by ionomycin. A simultaneous decrease in epifluorescence also supports the conclusion that vesicles fused with the plasma membrane and released their contents into the extracellular space, rather than they moved away to the cell interior out of TIRF microscopy range, which could potentially be the case with the decrease in TIRF signal only (38). In 4–5% of vesicles an initial increase in TIRF signal was followed by a decrease, which indicates that the stimulus-dependent exocytosis was preceded by docking.

To further investigate the mechanism of ATP release from astrocytes we employed a sniffer cell method with engineered HEK cells. This method has been successfully used to detect the release of glutamate from astrocytes (50); however it has not been used to study ATP release form astrocytes, yet. We transfected HEK-293T cells with a mutated form of $P2X_3$ receptor (D266A; Ref. 37), which drastically reduces receptor desensitization while retaining receptor affinity in low micromolar range (37). In HEK-293T cells a high degree of co-localization between EGFP and anti-$P2X_3$ antibody suggested expression of $P2X_3$ receptors. For patch-clamp experiments green fluorescent $P2X_3$-expressing HEK-293T cells lying in close vicinity of astrocytes or on top of them were chosen since the fast diffusion and the rapid hydrolysis of the astrocyte-derived ATP could greatly reduce the detection of ATP by sniffer cells. In resting conditions we observed random STICs with kinetic properties suggestive of their quantal origin. Thus, it seems likely that spontaneous ATP release from astrocytes could at least in part be vesicular. The kinetics of STICs were slower than those of

analogous events detected in $P2X_2$ receptor-expressing PC12 cells (26).

In TIRF studies, astrocyte stimulation triggered fusion of quinacrine-stained vesicles with the plasma membrane only 2–7 min later. This is consistent with the involvement of the relatively slow release mechanism in astrocytes compared with neurons (29, 39, 40, 51). As expected for regulated exocytosis, following glutamate stimulation of astrocytes the average frequency of STICs significantly increased. Because HEK-293T cells do not respond to glutamate directly, the increased frequency of recorded STICs suggests that we stimulated vesicular release of ATP from astrocytes. Furthermore, consistent with a key role of Ca^{2+} in exocytosis, in Ca^{2+}-free solution much fewer STICs were observed both in resting and glutamate-stimulated conditions. Our results are consistent with the observations by Pascual *et al.* (10), who showed ATP release from astrocytes to be dependent on the presence of intact SNARE proteins (involved in the exocytotic release mechanism) and also complement the results obtained by Coco *et al.* (14). Additionally, we confirmed the requirement of SNARE proteins in cargo release from quinacrine-stained vesicles by transfecting astrocytes with a construct to express the dominant-negative SNARE domain peptide. In transfected cells, the number of quinacrine-stained vesicle remained unaltered following ionomycin stimulation (supplemental Fig. S1). These results strongly suggest exocytotic cargo release from quinacrine-stained vesicles as considered previously (10, 14).

The present data collectively provided strong evidence for vesicular storage of ATP in astrocytes and offered the opportunity to examine the spontaneous and stimulated mobility of ATP-containing vesicles. Our results obtained by both imaging techniques and electrophysiological approaches indicate the presence of Ca^{2+}-dependent, exocytotic release of ATP from stimulated astrocytes. Because ATP is a major gliotransmitter involved in the propagation of calcium waves among astrocytes (2) and in the modulation of neuronal activity (10, 52, 53), the release mechanism reported in the current study may play a role in activity-dependent the relatively rapid delivery of the gliotransmitter ATP to the extracellular milieu as a signaling messenger for intercellular communication.

REFERENCES

1. Araque, A., Parpura, V., Sanzgiri, R. P., and Haydon, P. G. (1999) *Trends Neurosci.* **22,** 208–215
2. Haydon, P. G. (2001) *Nat. Rev. Neurosci.* **2,** 185–193
3. Newman, E. A. (2003) *Trends Neurosci.* **26,** 536–542
4. Fellin, T., Pascual, O., and Haydon, P. G. (2006) *Physiology* **21,** 208–215
5. Martin, D. L. (1992) *Glia* **5,** 81–94
6. Porter, J. T., and McCarthy, K. D. (1997) *Prog. Neurobiol.* **51,** 439–455
7. Evanko, D. S., Zhang, Q., Zorec, R., and Haydon, P. G. (2004) *Glia* **47,** 233–240
8. Kang, J., Jiang, L., Goldman, S. A., and Nedergaard, M. (1998) *Nat. Neurosci.* **1,** 683–692
9. Fellin, T., Pascual, O., Gobbo, S., Pozzan, T., Haydon, P. G., and Carmignoto, G. (2004) *Neuron* **43,** 729–743
10. Pascual, O., Casper, K. B., Kubera, C., Zhang, J., Revilla-Sanchez, R., Sul, J.-Y., Takano, H., Moss, S. J., McCarthy, K., and Haydon, P. G. (2005) *Science* **310,** 113–116
11. Lazarowski, E. R., Boucher, R. C., and Harden, T. K. (2003) *Mol. Pharmacol.* **64,** 785–795
12. Cotrina, M. L., Lin, J. H.-C., Alves-Rodrigues, A., Liu, S., Li, J., Azmi-Ghadimi, H., Kang, J., Naus, C. C. G., and Nedergaard, M. (1998) *Proc. Natl. Acad. Sci. U. S. A.* **95,** 15735–15740
13. Bal-Price, A., Moneer, Z., and Brown, G. C. (2002) *Glia* **40,** 312–323
14. Coco, S., Calegari, F., Pravettoni, E., Pozzi, D., Taverna, E., Rosa, P., Matteoli, M., and Verderio, C. (2003) *J. Biol. Chem.* **278,** 1354–1362
15. Arcuino, G., Lin, J. H.-C., Takano, T., Liu, C., Jiang, L., Gao, Q., Kang, J., and Nedergaard, M. (2002) *Proc. Natl. Acad. Sci. U. S. A.* **99,** 9840–9845
16. Stout, C. E., Constantin, J. L., Naus, C. C., and Charles, A. C. (2002) *J. Biol. Chem.* **277,** 10482–10488
17. Queiroz, G., Gebicke-Haerter, P. J., Schobert, A., Starke, K., and von Kugelgen, I. (1997) *Neuroscience* **78,** 1203–1208
18. Anderson, C. M., Bergher, J. P., and Swanson, R. A. (2004) *J. Neurochem.* **88,** 246–256
19. Abraham, E. H., Prat, A. G., Gerweck, L., Seneveratne, T., Arceci, R. J., Kramer, R., Guidotti, G., and Cantiello, H. F. (1993) *Proc. Natl. Acad. Sci. U. S. A.* **90,** 312–316
20. Schwiebert, E. M., Egan, M. E., Hwang, T. H., Fulmer, S. B., Allen, S. S., Cutting, G. R., and Guggino, W. B. (1995) *Cell* **81,** 1063–1073
21. Parpura, V., Fang, Y., Basarsky, T. A., Jahn, R., and Haydon, P. G. (1995) *FEBS Lett.* **377,** 489–492
22. Montana, V., Ni, Y., Sunjara, V., Hua, X., and Parpura, V. (2004) *J. Neurosci.* **24,** 2633–2642
23. Wilhelm, A., Volknandt, W., Langer, D., Nolte, C., Kettenmann, H., and Zimmermann, H. (2004) *Neurosci. Res.* **48,** 249–257
24. Zhang, Q., Pangršič, T., Kreft, M., Kržan, M., Li, N., Sul, J. Y., Halassa, M., Van Bockstaele, E., Zorec, R., and Haydon, P. G. (2004) *J. Biol. Chem.* **279,** 12724–12733
25. Zimmermann, H. (1994) *Trends Neurosci.* **17,** 420–426
26. Fabbro, A., Skorinkin, A., Grandolfo, M., Nistri, A., and Giniatullin, R. (2004) *J. Physiol.* **560,** 505–517
27. Grandolfo, M., and Nistri, A. (2005) *Neuroreport* **16,** 381–385
28. Kržan, M., Stenovec, M., Kreft, M., Pangršič, T., Grilc, S., Haydon, P. G., and Zorec, R. (2003) *J. Neurosci.* **23,** 1580–1583
29. Kreft, M., Stenovec, M., Rupnik, M., Grilc, S., Kržan, M., Potokar, M., Pangršič, T., Haydon, P. G., and Zorec, R. (2004) *Glia* **46,** 437–445
30. Potokar, M., Kreft, M., Li, L., Andersson, D., Pangršič, T., Chowdhury, H. H., Pekny, M., and Zorec, R. (2006) *Traffic* **8,** 12–20
31. Bodin, P., and Burnstock, G. (2001) *J. Cardiovasc. Pharmacol.* **38,** 900–908
32. Pangršič, T., Potokar, M., Haydon, P. G., Zorec, R., and Kreft, M. (2006) *J. Neurochem.* **99,** 514–523
33. Axelrod, D. (2003) *Methods Enzymol.* **361,** 1–33
34. Kolikova, J., Afzalov, R., Giniatullina, A., Surin, A., Giniatullin, R., and Khiroug, L. (2006) *Brain Cell Biol.* **35,** 75–86
35. Potokar, M., Kreft, M., Pangršič, T., and Zorec, R. (2005) *Biochem. Biophys. Res. Commun.* **329,** 678–683
36. Wacker, I., Kaether, C., Kromer, A., Migala, A., Almers, W., and Gerdes, H. H. (1997) *J. Cell Sci.* **110,** 1453–1463
37. Fabbretti, E., Sokolova, E., Masten, L., D'Arco, M., Fabbro, A., Nistri, A., and Giniatullin, R. (2004) *J. Biol. Chem.* **279,** 53109–53115
38. Striedinger, K., Meda, P., and Scemes, E. (2007) *Glia* **55,** 652–662
39. Araque, A., Sanzgiri, R. P., Parpura, V., and Haydon, P. G. (1998) *J. Neurosci.* **18,** 6822–6829
40. Pankratov, Y., Lalo, U., Krishtal, O., and Verkhratsky, A. (2003) *Mol. Cell. Neurosci.* **24,** 842–849
41. Sokolova, E., Skorinkin, A., Fabbretti, E., Masten, L., Nistri, A., and Giniatullin, R. A. (2004) *Br. J. Pharmacol.* **141,** 1048–1058
42. Jarvis, M. F., Burgard, E. C., McGaraughty, S., Honore, P., Lynch, K., Brennan, T. J., Subieta, A., Van Biesen, T., Cartmell, J., Bianchi, B., Niforatos, W., Kage, K., Yu, H., Mikusa, J., Wismer, C. T., Zhu, C. Z., Chu, K., Lee, C. H., Stewart, A. O., Polakowski, J., Cox, B. F., Kowaluk, E., Williams, M., Sullivan, J., and Faltynek, C. (2002) *Proc. Natl. Acad. Sci. U. S. A.* **99,** 17179–17184
43. Simonetti, M., Fabbro, A., D'Arco, M., Zweyer, M., Nistri, A., Giniatullin, R., and Fabbretti, E. (2006) *Mol. Pain* **2,** 11
44. North, R. A. (2002) *Physiol. Rev.* **82,** 1013–1067
45. Schliwa, M., and Woehlke, G. (2003) *Nature* **422,** 759–765

46. Schutz, G. J., Axmann, M., Freudenthaler, S., Schindler, H., Kandror, K., Roder, J. C., and Jeromin, A. (2004) *Microsc. Res. Tech.* **63,** 159–167
47. Ng, Y. K., Lu, X., and Levitan, E. S. (2002) *J. Physiol.* **542,** 395–402
48. Han, W., Ng, Y. K., Axelrod, D., and Levitan, E. S. (1999) *Proc. Natl. Acad. Sci. U. S. A.* **96,** 14577–14582
49. Shakiryanova, D., Tully, A., Hewes, R. S., Deitcher, D. L., and Levitan, E. S. (2005) *Nat. Neurosci.* **8,** 173–178
50. Pasti, L., Zonta, M., Pozzan, T., Vicini, S., and Carmignoto, G. (2001) *J. Neurosci.* **21,** 477–484
51. Stenovec, M., Kreft, M., Poberaj, I., Betz, W. J., and Zorec, R. (2004) *FASEB J.* **18,** 1270–1272
52. Haydon, P. G., and Carmignoto, G. (2006) *Physiol. Rev.* **86,** 1009–1031
53. Zhang, J. M., Wang, H. K., Ye, C. Q., Ge, W., Chen, Y., Jiang, Z. L., Wu, C. P., Poo, M. M., and Duan, S. (2003) *Neuron* **40,** 971–982

Exocytotic Release of ATP from Cultured Astrocytes

Tina Pangrsic, Maja Potokar, Matjaz Stenovec, Marko Kreft, Elsa Fabbretti, Andrea Nistri, Evgeny Pryazhnikov, Leonard Khiroug, Rashid Giniatullin and Robert Zorec

J. Biol. Chem. 2007, 282:28749-28758.
doi: 10.1074/jbc.M700290200 originally published online July 12, 2007
